Article

Kinematic and Dynamic Modelling for a Class of Hybrid Robots Composed of *m* Local Closed-Loop Linkages Appended to an *n*-Link Serial Manipulator

Anh My Chu [1,*]**, Cong Dinh Nguyen** [1]**, Minh Hoan Vu** [2]**, Xuan Bien Duong** [3]**, Tien Anh Nguyen** [4] **and Chi Hieu Le** [5]

[1] Institute of Simulation Technology, Le Quy Don Technical University, Ha Noi 10000, Vietnam; dinhnc@mta.edu.vn
[2] Department of Mechanical Engineering, Le Quy Don Technical University, Ha Noi 10000, Vietnam; hoanvm92@gmail.com
[3] Department of Aerospace, Le Quy Don Technical University, Ha Noi 10000, Vietnam; duongxuanbien@lqdtu.edu.vn
[4] Department of Physics, Le Quy Don Technical University, Ha Noi 10000, Vietnam; anhnt@lqdtu.edu.vn
[5] Faculty of Engineering and Science, University of Greenwich, Kent ME4 4TB, UK; C.H.Le@greenwich.ac.uk
[*] Correspondence: myca@lqdtu.edu.vn

Featured Application: The systematic and generic method proposed in this study for the kinematic design and dynamic modelling for a class of complex hybrid robots is useful and applicable for the development of new hybrid robot products. Based on the proposed method, the mechanism of a new hybrid robot can be synthesized and analysed effectively; the dynamic model and control law of a complex robot can be formulated and simulated in a simplified and effective manner.

Abstract: Recently, more and more hybrid robots have been designed to meet the increasing demand for a wide spectrum of applications. However, development of a general and systematic method for kinematic design and dynamic analysis for hybrid robots is rare. Most publications deal with the kinematic and dynamic issues for individual hybrid robots rather than any generalization. Hence, in this paper, we present a novel method for kinematic and dynamic modelling for a class of hybrid robots. First, a generic scheme for the kinematic design of a general hybrid robot mechanism is proposed. In this manner, the kinematic equation and the constraint equations for the robot class are derived in a generalized case. Second, in order to simplify the dynamic modelling and analysis of the complex hybrid robots, a Lemma about the analytical relationship among the generalized velocities of a hybrid robot system is proven in a generalized case as well. Last, examples of the kinematic and dynamic modelling of a newly designed hybrid robot are presented to demonstrate and validate the proposed method.

1. Introduction

Generally, the robotic mechanisms can be categorized into three main groups: the open-loop mechanism, the closed-loop mechanism and the hybrid mechanism. A robot of the first group is usually designed with an end-effector connected to a fixed base by means of a single serial kinematic chain. Meanwhile, each robot of the second group is a mechanism which is usually composed of a moving end-effector connected to a fixed base by at least two kinematic chains, such as the parallel

robots. A hybrid manipulator is a mechanism which is usually composed of some open-loop kinematic chains combined with some closed-loop linkages [1–34].

The main advantages of the serial robots are the large workspace, the high dexterity of the end-effector and the large non-singular range of the joint variables. However, the robots of this group suffer from several drawbacks, such as relatively low stiffness and accuracy, low nominal load/weight ratio and heavy structure [21]. Therefore, in the last decades, several types of robots having closed-loop kinematic chains have been investigated in order to obtain better kinematic performances. The main advantages of these robots are low weight, compact structure, better accuracy and stiffness. Nevertheless, this robot group also have some disadvantages, such as a small workspace, a complex mechanical design and a complex procedure for dynamic modelling and control. For these reasons, in recent years, great attention has been paid to the development of hybrid robots which have combined advantages of the serial robots and the closed-loop architectures. More and more hybrid robots are designed and developed to meet the increasing demand for a wide spectrum of hybrid robotic applications [10–30].

In practice, the hybrid robots have been designed in a large variety of kinematic configurations and structures, and they can be classified into three main classes as follows:

The first class (Class I) includes all the hybrid robots whose structure has several parallel modules connected in series [1–10] (Figure 1a).

(a) **(b)** **(c)**
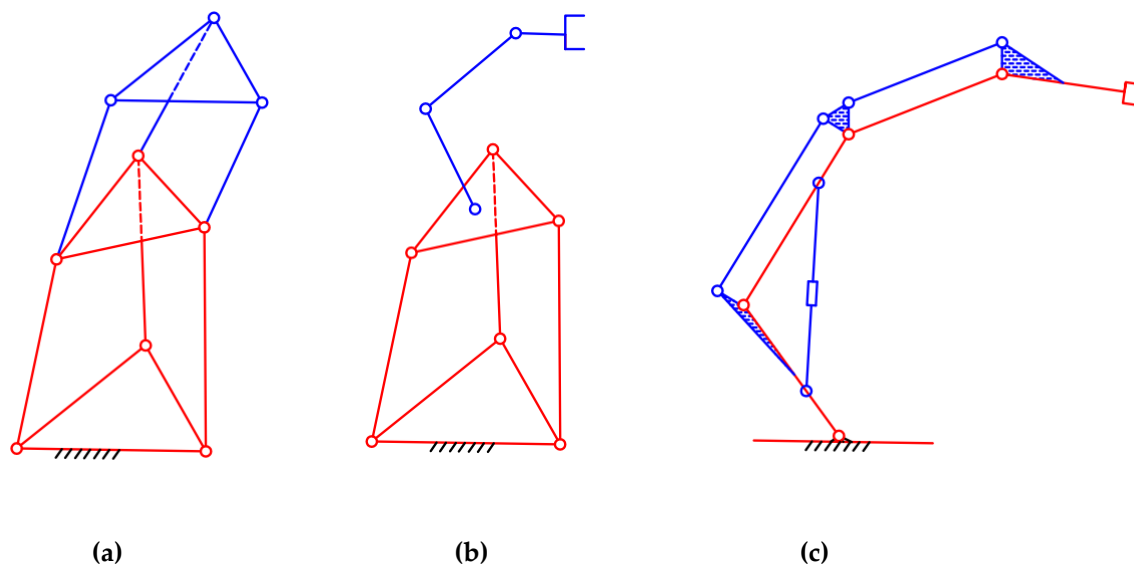
Figure 1. Three main classes of the hybrid robots: (**a**) Class I; (**b**) Class II and (**c**) Class III

Class II consists of the hybrid robots which have a basic parallel module combined with a serial manipulator [11–24] (Figure 1b).

Class III is a family of the hybrid robots which are composed of some local closed-loop chains appended to a main serial mechanism [25–33] (Figure 1c).

It is clearly seen that the main architecture of a hybrid robot Class I or II is a parallel mechanism. Other parallel modules or serial links are connected to such the main structure to complete a hybrid serial-parallel robot.

Different from the robots Class I and II, each hybrid robot Class III is usually designed with a serial module as the main structure of a robot. To provide with desirable mechanical advantages for a hybrid robot, some local closed-loop mechanisms are added to the main serial module. For example, when designing manipulators which suffer a heavy payload and operate in a large workspace, parallelograms were added and hydraulic cylinders were used for driving some revolute joints of the manipulators [26,28–31]. The addition of parallelograms to the main arm is to increase the rigidity of the robot, and also to restrict the orientation of the end- effector as desired. The use of the hydraulic

cylinders is to increase the structural stiffness and to avoid the counterweights for the robot structure. The parallelograms and cylinders and other links of the serial arm naturally compose local closed loops of the entire robot mechanism. Other examples of using local closed-loop linkages to optimize the design and control for a robot can be found in [26–34].

In recent decades, a huge number of hybrid robot prototypes and products have been designed and developed [10–30]. The dynamic modelling and control for some of these complex robots have been addressed as well. However, to develop a generic method for formulating the dynamic model of a generalized hybrid robot mechanism is challenging.

In the literature, there have been efforts that focused on the kinematic modelling of the hybrid robots Class I [1–5]. The kinematic modelling and analysis of two serially connected parallel mechanisms were investigated in [1]. In [2], the kinematic redundancy issue of a serial-parallel manipulator was addressed. The Screw theory and the Jacobian approach were applied for the kinematic modelling of a serial-parallel robot [3,4]. In particular, the dynamics and the structural stiffness models of some specific hybrid robots Class I were formulated and analysed [6–9].

There have also been attempts working on the modelling and analysis of the hybrid robots Class II [11–21]. A real-time implementation of path planning, trajectory generation, and servo control for a hybrid manipulation was presented in [11]. The kinematic modelling, the kinematic design, the workspace modelling and other aspects related to the kinematics of the hybrid robots Class II were studied [12–17]. The dynamic modelling and analysis of the robots Class II were also investigated [18,19]. In addition, the structural synthesis and the stiffness of the hybrid robots of this class were studied [20–22].

Apart from the aforementioned works, there have been investigations that emphasized on design and development of the hybrid robots Class III [25–33]. A valuable comparison of the conventional serial robot architectures and the hybrid robots Class III was presented in [34]. In the research [25], some theoretical issues related to the kinematic modelling of multi closed-loop mechanisms were addressed. In addition, some closed-form solutions to the kinematics problem of individual hybrid robots Class III were presented in [26–28]. These solutions played an important role in validating the design of the robots. The workspace and mobility analysis were also investigated in [28,29]. Other aspects related to the design analysis of heavy-duty robots were presented in [30,31]. The control issues were studied in [32,33]. It is noticeable that the dynamic modelling of a hybrid manipulator Class III (forestry robot) was investigated in [33]. However, the effects of the local closed-loops on the dynamic responses of this robotic system were overlooked.

Most of the efforts working on the hybrid robots Class III mainly focused on the design and control of some individual robots for the kinematical aspects. Though the dynamic modelling of the robots was addressed in a few researches, e.g., [33], however, the mass and inertia of the local closed-loop linkages that have significant effects on the robot motion were neglected; the geometrical and kinematical constraints due to the presence of the local closed-loop linkages were usually ignored. Moreover, little attention has been paid to the development of a general method for the kinematic and dynamic modelling of this robot class. Therefore, in this paper, a new method for designing the kinematic chain and formulating the dynamic model of the hybrid robots is developed. First, a generic scheme for the kinematic design of a generalized hybrid robot mechanism is proposed. In this scheme, the generalized hybrid mechanism is synthesized with m local closed-loop linkages appended to a general n-link serial manipulator. Each locally closed linkage is regarded as a four bars mechanism which is made up of two successive links of the main serial arm, and other two added links. Second, the kinematic equation for the generalized hybrid mechanism and constraint equations for the closed loops are derived in a generalized case. Third, a Lemma about the relationship among the generalized velocities of the hybrid robots is proven, which is useful for transforming the dynamic equation and constraint equations into a minimal and compact form. Last, the kinematic and dynamic modelling of a real robot prototype are presented to demonstrate and validate the proposed method. It is shown clearly that, since the kinematic and dynamic modelling of a hybrid robot take into account the constraint equations and the

dynamic effects of all the local closed loops, the kinematics and dynamics models of a hybrid robot are formulated in a better and more accurate manner. Therefore, the method proposed in this study is advantageous and plays a crucial role in the development of hybrid robot products.

2. Kinematics of a Generalized Mechanism for The Hybrid Robots Class III

Let us consider a manipulator which is designed with n serial links $\{l_i\}_{i=1 \div n}$ and m local closed-loop mechanisms $\{\Theta_k\}_{k=1 \div m}$, ($m < n \leq 6$) as shown in Figure 2. The serial chain of n links is the main mechanism of the robot arm, and the closed-loop mechanisms are designed as sub-mechanisms appended to the main one. The degree of freedom number (DOFs) of the designed robot equals the DOFs of the main mechanism, *n*. The presence of the local closed-loop mechanisms does not change the DOFs of the robot.
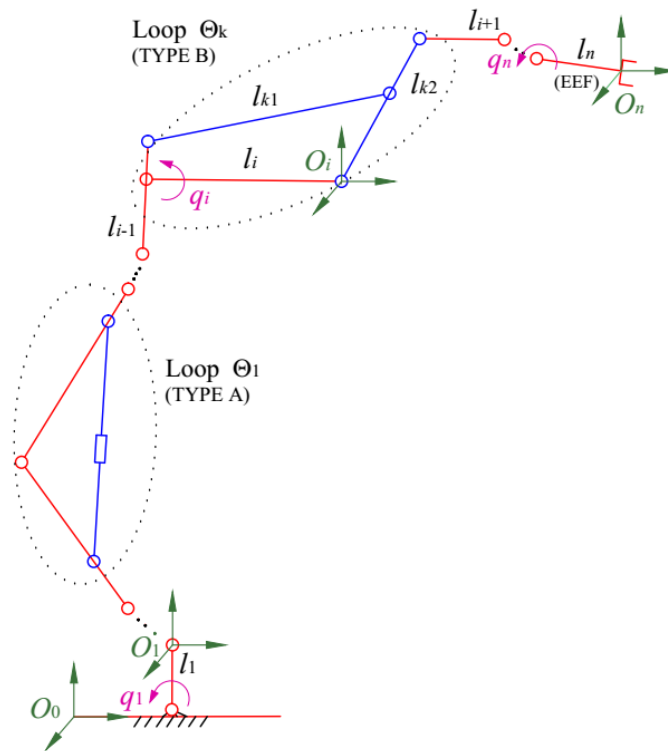

Figure 2. A generalized configuration of the hybrid robots Class III.

Each local closed mechanism Θ_k is designed with two successive links l_{i-1} and l_i of the main arm and other two appended links l_{k_1} and l_{k_2}. See Figures 2 and 3. In other words, each local closed-loop mechanism is designed as a four bar linkage which is composed of the links l_{i-1}, l_i, l_{k_1} and l_{k_2}. In a local closed chain linkage, the link l_{i-1} is a local base link, and the remained links l_i, l_{k_1} and l_{k_2} move relative to the base link l_{i-1}.

As shown in Figure 3, there exists four types of the local closed-loops, Type A, B, C and D, which can be designed by combining a couple of successive links l_{i-1} and l_i of the main arm and other two links l_{k_1} and l_{k_2} added to the robot architecture.

In a local closed-loop Type A (Figure 3a), the two links l_{k_1} and l_{k_2} are added to the main arm, and the output link is a link l_i. Meanwhile in Type B (Figure 3b), the two links l_{k_1} and l_{k_2} are inserted in between the links l_{i-1} and l_i, but the output link is the link l_{k_2}. When a loop Type B is added to the main kinematic chain, the link l_{k_2} is inserted in between l_i and l_{i+1}.
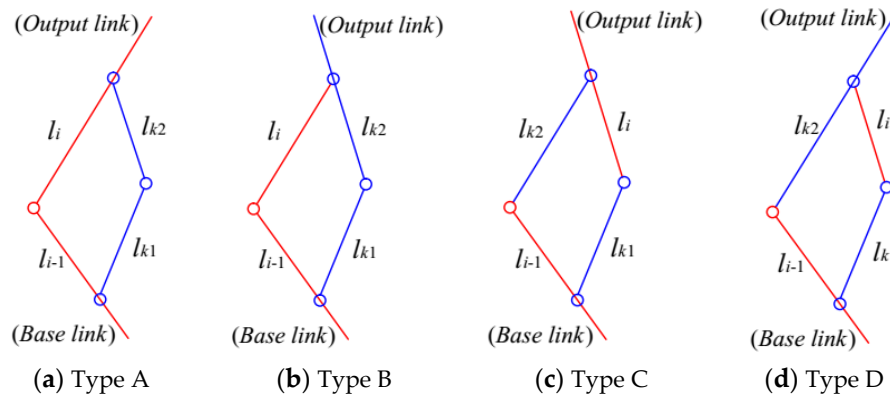
Figure 3. Four types of the local closed-loops.

When the two links l_{k_1} and l_{k_2} are not connected together, there exists two more combinations of the links l_{i-1}, l_i, l_{k_1} and l_{k_2} as shown in Figure 3c,d. In a loop Type C, the output link is l_i, meanwhile in Type D, the output link is l_{k_2}.

For all four types of the local linkages, the base link is l_{i-1}, and the formation of all the closed-loop mechanisms does not change the DOFs of the robot.

Let us consider the main kinematic chain of the hybrid robot. In Figure 2, $O_0 \equiv (O_0 x_0 y_0 z_0)$ is the reference frame, and $O_1 \equiv (O_1 x_1 y_1 z_1)$ to $O_n \equiv (O_n x_n y_n z_n)$ are the local coordinate systems which are attached to all the links of the main arm. Let us denote $\mathbf{q} = \begin{bmatrix} q_1 & q_2 & q_3 & \dots & q_n \end{bmatrix}^T$ as the vector of joint variables on the main arm, correspondingly.

As usual, the geometric and kinematic parameters of a link l_i are denoted as θ_i, d_i, a_i and α_i. By using the Denavit–Hartenberg notation, the transformation matrix for the end-effector (EEF) can be calculated as follows:

$$\mathbf{H}_{0E} = \mathbf{H}_{01}(q_1)\mathbf{H}_{12}(q_2)\mathbf{H}_{23}(q_3)\dots\mathbf{H}_{(n-1)n}(q_n) \tag{1}$$

where $\mathbf{H}_{(i-1)i}(q_i)$ is the transformation matrix for a link l_i.

In other words, $\mathbf{H}_{0E}$ can be expressed as follows:

$$\mathbf{H}_{0E} = \begin{bmatrix} \mathbf{A}(\mathbf{q}) & \mathbf{r}(\mathbf{q}) \\ 0 & 1 \end{bmatrix} \tag{2}$$

where $\mathbf{A}(\mathbf{q})$ is the rotation matrix, and $\mathbf{r}(\mathbf{q})$ is the translation vector for the EEF. Equation (2) describes the kinematic relationship of the robot. If we denote $\mathbf{p}_E = \begin{bmatrix} x_E & y_E & z_E & \alpha & \beta & \gamma \end{bmatrix}^T$ as the posture of the EEF in O_0, where $\begin{bmatrix} x_E & y_E & z_E \end{bmatrix}^T$ is the position and $\begin{bmatrix} \alpha & \beta & \gamma \end{bmatrix}^T$ the orientation of the EEF, the kinematic equation can be written as follows:

$$\mathbf{p}_E = \mathbf{f}(\mathbf{q}) \tag{3}$$

Let us consider all the local-closed loops Type A, B, C or D, which can be added to the main kinematic chain, as shown in Figure 3. The presence of a closed chain Type A does not change Equation (1). However, Equation (1) must be recalculated if a closed loop Type B, C or D is designed for the robot.

For a local linkage Type B, since a link l_{k_2} is inserted in between l_i and l_{i+1}, the transformation matrix $\mathbf{H}_{i(i+1)}(q_{i+1})$ in Equation (1) must be recalculated as follows:

$$\mathbf{H}_{i(i+1)}(q_{i+1}) = \mathbf{H}_{ik_1}(q_{k_1})\mathbf{H}_{k_1 k_2}(q_{k_2})\mathbf{H}_{k_2(i+1)}(q_{i+1}) \tag{4}$$

For a local linkage Type C and D, the matrix $\mathbf{H}_{(i-1)i}(q_i)$ is replaced by the following matrix:

$$\mathbf{H}_{(i-1)i}(q_i) = \mathbf{H}_{(i-1)k_1}(q_{k_1})\mathbf{H}_{k_1 i}(q_i) \tag{5}$$

In particular, for a linkage Type D, not only $\mathbf{H}_{(i-1)i}(q_i)$ is re-calculated with Equation (5), but also the matrix $\mathbf{H}_{i(i+1)}(q_{i+1})$ must be re-calculated as follows:

$$\mathbf{H}_{i(i+1)}(q_{i+1}) = \mathbf{H}_{(i-1)k_2}(q_{k_2})\mathbf{H}_{k_2(i+1)}(q_{i+1}) \tag{6}$$

Note that the variables q_{k_1} and q_{k_2} in Equations (4)–(6) can be determined with respect to q_i via the two constraint equations of a corresponding closed-loops Θ_k, which will be presented later in the next section.

Constraint equations

Different from the formulation of the kinematics model for a serial robot, the formulation of the hybrid kinematics models of the hybrid robots Class III must take into account the constraints due to the presence of the local closed-loops.

As discussed before, each linkage Θ_k includes two sub-kinematic chains that move relative to the base link. For example, as shown in Figure 4a, the first sub-chain of a linkage Type A is the link l_i, and the second sub-chain includes the two link l_{k_1} and l_{k_2}. Obviously, the two sub-chains of a linkage are closed at an intersection point M (see Figure 4).

(a) Type A   **(b)** Type B   **(c)** Type C   **(d)** Type D
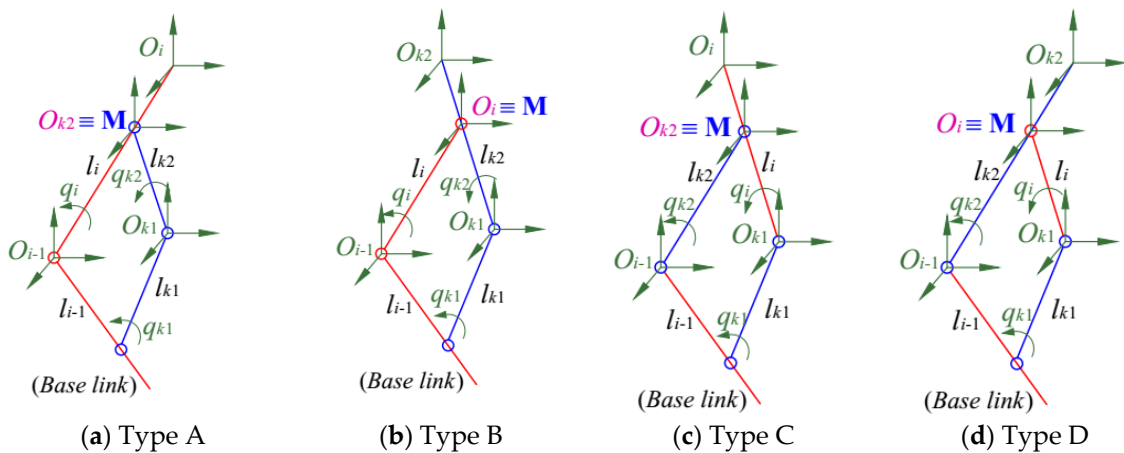
Figure 4. The closed kinematic chain of the local linkages.

In order to derive the constraint equation for a loop Θ_k, the position of the point M are determined along the two sub-chains.

On one hand, the point M, $\mathbf{r}_M^i = \begin{bmatrix} x_M^i & y_M^i & z_M^i & 1 \end{bmatrix}^T$ represented in the coordinate O_i of the link l_i, can be determined via the position and orientation of the link l_i that can be calculated relative to the base link l_{i-1}. On the other hand, the point M, $\mathbf{r}_M^{k_2} = \begin{bmatrix} x_M^{k_2} & y_M^{k_2} & z_M^{k_2} & 1 \end{bmatrix}^T$ expressed in O_{k_2}, can be calculated through the position and orientation of the link l_{k_2}. Consequently, the constraint equation for a loop Type A and B can be yielded as follows:

$$\mathbf{H}_{(i-1)i}(q_i) \cdot \mathbf{r}_M^i = \mathbf{H}_{(i-1)k_1}(q_{k_1}) \cdot \mathbf{H}_{k_1 k_2}(q_{k_2}) \cdot \mathbf{r}_M^{k_2} \tag{7}$$

For a loop Type C and D the constraint equation can be written as follows:

$$\mathbf{H}_{(i-1)k_2}(q_{k_2}) \cdot \mathbf{r}_M^{k_2} = \mathbf{H}_{(i-1)k_1}(q_{k_1}) \cdot \mathbf{H}_{k_1 i}(q_i) \cdot \mathbf{r}_M^i \tag{8}$$

Note that, for a closed-loop Type A or Type C, the point M coincides the point O_{k_2}, thus $\mathbf{r}_M^{k_2} = \begin{bmatrix} 0 & 0 & 0 & 1 \end{bmatrix}^T$. In addition, for a closed-loop Type B or Type D, $\mathbf{r}_M^i = \begin{bmatrix} 0 & 0 & 0 & 1 \end{bmatrix}^T$.

In essence, Equations (7) and (8) can be rewritten as three constraint equations corresponding to three axes of the coordinate system O_{i-1}. However, among such the three constraint equations, there exist only two independent ones, since all the closed-loops under consideration are planar four bar linkages. As a consequence, corresponding to a loop Θ_k, the two independent constraint equations can be written as follows:

$$\mathbf{f}_k\left(q_i, q_{k_1}, q_{k_2}\right) = \begin{bmatrix} f_{k_1}\left(q_i, q_{k_1}, q_{k_2}\right) \\ f_{k_2}\left(q_i, q_{k_1}, q_{k_2}\right) \end{bmatrix} = 0 \tag{9}$$

For every local linkage, only one joint variable among q_i, q_{k_1} and q_{k_2} is independent. The kinematic relationships among q_i, q_{k_1} and q_{k_2} are determined via the two constraint equations, Equation (9), for each closed-loop Θ_k. Therefore, in the case that, instead of q_i, the variable q_{k_1} or q_{k_2} is selected as the independent joint variable of Θ_k, the variable q_i in the transformation matrix $\mathbf{H}_{(i-1)i}\left(q_i\right)$ in Equation (1) must be changed by the variable $q_i = h_k\left(q_{k_1}\right)$ or $q_i = g_k\left(q_{k_2}\right)$, respectively, where the functions h_k and g_k can be determined with respect to the kinematic relationships among q_i, q_{k_1} and q_{k_2}.

3. Dynamic Modelling of the Hybrid Robots Class III

$\mathbf{u} = \begin{bmatrix} u_1 & u_2 & u_3 & \dots & u_n \end{bmatrix}^T$ is the vector of n independent generalized coordinates which are selected among n joint variables $\{q_i\}_{i=1 \div n}$ of the main arm, and $2 \times m$ joint variables $\{q_{k_1}, q_{k_2}\}_{k=1 \div m}$ of m closed-loops. In other words, $\mathbf{u}$ is the vector of all active joint variables.

$\mathbf{z} = [z_1 \ z_2 \ \dots \ z_{2m}]^T$ is the vector of $2m$ dependent generalized coordinates.

$\mathbf{s} = \begin{bmatrix} \mathbf{u} & \mathbf{z} \end{bmatrix}^T$ is the vector of all $(n + 2m)$ generalized coordinates of the robot system.

$\mathbf{f} = \begin{bmatrix} f_{11} & f_{12} & \dots & f_{m1} & f_{m2} \end{bmatrix}^T$ is the vector of $2m$ constraint equations.

$$\boldsymbol{\tau} = \begin{bmatrix} \underbrace{\tau_1 \quad \tau_2 \quad \dots \quad \tau_n}_{n} & \underbrace{0 \quad \dots \quad 0}_{2m} \end{bmatrix}^T$$ is the vector of applied torques/forces.

By using the Lagrangian formulation, the equations of motion including constraint equations for the robot can be written as follows:

$$\begin{cases} \mathbf{M}(\mathbf{s}, t)\ddot{\mathbf{s}} + \mathbf{C}\left(\mathbf{s}, \dot{\mathbf{s}}, t\right)\dot{\mathbf{s}} + \mathbf{g}(\mathbf{s}, t) + \mathbf{J}_s^T \lambda = \tau(t) \\ \mathbf{f}(\mathbf{s}, t) = 0 \end{cases} \tag{10}$$

Note that the size of the global matrices $\mathbf{M}(\mathbf{s}, t)$ and $\mathbf{C}\left(\mathbf{s}, \dot{\mathbf{s}}, t\right)$ is $(n + 2m) \times (n + 2m)$. The global mass matrix $\mathbf{M}(\mathbf{s}, t)$ must be formulated with respect to all the links of the robot including n links of the serial chain and $2m$ links added to m local closed-loops.

The global mass matrix is calculated as follows:

$$\mathbf{M}(\mathbf{s}, t) = \sum_{j=1}^{n+2m} \left(m_j \mathbf{J}_{T_j}^T \mathbf{J}_{T_j} + \mathbf{J}_{R_j}^T \mathbf{I}_j \mathbf{J}_{R_j} \right) \tag{11}$$

where m_j and $\mathbf{I}_j$ are the mass and inertia of a link j. The translational and rotational Jacobian matrices are calculated as $\mathbf{J}_{T_j} = \frac{\partial \mathbf{r}_{Cj}}{\partial \mathbf{s}}$ and $\mathbf{J}_{R_j} = \frac{\partial \boldsymbol{\omega}_j}{\partial \dot{\mathbf{s}}}$, where $\mathbf{r}_{Cj}$ is the centre of mass, and $\boldsymbol{\omega}_j$ is the angular velocity of a link j, respectively.

The Coriolis and centrifugal matrix $\mathbf{C}\left(\mathbf{s}, \dot{\mathbf{s}}, t\right)$ is calculated by using Cristoffel notation.

The matrix $\mathbf{g}(\mathbf{s}, t)$ is calculated as follows:

$$\mathbf{g}(\mathbf{s}, t) = \left[\frac{\partial \Pi}{\partial \mathbf{s}}\right]^T \tag{12}$$

where the total potential energy of the entire system is calculated as

$$\Pi = \sum_{j=1}^{n+2m} m_j \mathbf{g}^T \mathbf{r}_{Cj} \tag{13}$$

The Jacobian matrix $\mathbf{J}_s$ is derived with respect to $2m$ constraint equations as $\mathbf{J}_s = \frac{\partial \mathbf{f}}{\partial \mathbf{s}}$, and $\lambda = \begin{bmatrix} \lambda_1 & \lambda_2 & \dots & \lambda_{2m} \end{bmatrix}^T$ is the vector of $2m$ Lagrangian Multipliers.

It is clear that the system of DAE equations seen in Equation (11) consists of $(n + 2m)$ differential equations of second order and $2m$ constraint equations $\mathbf{f}(\mathbf{s}, t) = 0$. Moreover, Equation (10) has not only n independent variables $\mathbf{u}$, but also $2m$ dependent variables $\mathbf{z}$ and $2m$ unknown Lagrangian Multipliers λ. Therefore, if using this complex system of DAEs to analyse the dynamics behaviour and to design a control law for the robot, the time complexity of the formulation and computation will be increased dramatically. For this reason, it is necessary to transform Equation (10) into a more compact form in which the Lagrangian Multipliers λ should be cancelled, and the number of the differential equations is minimized.

By using the following Lemma, $(n + 2m)$ differential equations of second order, Equation (10), can be transformed into only n differential equations of second order which are expressed in terms of only n independent generalized coordinates, not including $2m$ Lagrangian Multipliers $\lambda = \begin{bmatrix} \lambda_1 & \lambda_2 & \dots & \lambda_{2m} \end{bmatrix}^T$.

Lemma. *Consider a generalized hybrid robot mechanism Class III which has n independent joint variables* $\mathbf{u} = \begin{bmatrix} u_1 & u_2 & u_3 & \dots & u_n \end{bmatrix}^T$ *and 2m dependent joint variables* $\mathbf{z} = [z_1\, z_2\, \dots\, z_{2m}]^T$. *The relationship between $\mathbf{u}$ and $\mathbf{z}$ is expressed as* $\dot{\mathbf{s}} = \begin{bmatrix} \dot{u} & \dot{z} \end{bmatrix}^T = R\dot{u}$, *in which the matrix R is explicitly calculated as* $R = \begin{bmatrix} E \\ -J_z^{-1}J_u \end{bmatrix}$, *where E is an identity matrix of appropriate dimension,* $J_u = \frac{\partial f}{\partial u}$ *and* $J_z = \frac{\partial f}{\partial z}$, *where* $f(\mathbf{s}, t) = 0$ *is the constraint equation.*

As a consequence of this Lemma, the following important relationships, Equations (14) and (15), can be proved easily.

$$\mathbf{R}^T \mathbf{J}_s^T = 0 \tag{14}$$

$$\ddot{\mathbf{s}} = \mathbf{R}\ddot{\mathbf{u}} + \dot{\mathbf{R}}\dot{\mathbf{u}} \tag{15}$$

In Equation (14), the Jacobian matrix $\mathbf{J}_s$ can be expressed as follows:

$$\begin{aligned} \mathbf{J}_s &= \frac{\partial \mathbf{f}}{\partial \mathbf{s}} \\ &= \begin{bmatrix} \frac{\partial \mathbf{f}}{\partial \mathbf{u}} & \frac{\partial \mathbf{f}}{\partial \mathbf{z}} \end{bmatrix} = \begin{bmatrix} \mathbf{J}_u & \mathbf{J}_z \end{bmatrix} \end{aligned} \tag{16}$$

Note that Equations (14) and (15) play a very important role in transforming the complex system Equation (10) into a minimal form. With respect to Equations (14) and (15), multiplying $\mathbf{R}^T$ with both sides of Equation (10) yields

$$\overline{\mathbf{M}}(\mathbf{s}, t)\ddot{\mathbf{u}} + \overline{\mathbf{C}}(\mathbf{s}, \dot{\mathbf{s}}, t)\dot{\mathbf{u}} + \overline{\mathbf{G}}(\mathbf{s}, t)\mathbf{u} = \tau_\mathbf{q}(t) \tag{17}$$

where

$\overline{\mathbf{M}} = \mathbf{R}^T \mathbf{M}(\mathbf{s}, t)\mathbf{R}, \overline{\mathbf{C}} = \mathbf{R}^T \big(\mathbf{M}(\mathbf{s}, t)\dot{\mathbf{R}} + \mathbf{C}(\mathbf{s}, \dot{\mathbf{s}}, t)\mathbf{R} \big), \overline{\mathbf{G}} = \mathbf{R}^T \mathbf{g}(\mathbf{s}, t)$, and $\tau_\mathbf{q} = \mathbf{R}^T \tau(t)$.

Different from the complex ADEs system in Equation (10), which has $n + 2m$ differential equations with the presence of $2m$ dependent variables $\mathbf{z}$, and $2m$ unknown Lagrangian Multipliers λ, the minimal form of the dynamic equation, Equation (17), consists of only n differential equations which are expressed for n independent generalized coordinates $\mathbf{u}$ only. Moreover, the matrix form of Equation (17) is similar

to the form of any dynamic equation that is usually written for a conventional industrial robot. Hence, by using Equation (17), the dynamic analysis and control law computation for any complex hybrid robot Class III can be implemented in an effective and simplified manner.

Proof of the Lemma. Taking a time derivative of the constraint equation $\mathbf{f}(\mathbf{s}, t) = 0$ yields

$$\mathbf{J}_s\dot{\mathbf{s}} = 0 \tag{18}$$

Substituting Equation (16) into Equation (18) obtains

$$\mathbf{J}_u\dot{\mathbf{u}} + \mathbf{J}_z\dot{\mathbf{z}} = 0 \tag{19}$$

Rewriting the relationship $\dot{\mathbf{s}} = \begin{bmatrix} \dot{\mathbf{u}} & \dot{\mathbf{z}} \end{bmatrix}^T = \mathbf{R}\dot{\mathbf{u}}$ in the following form:

$$\begin{aligned} \dot{\mathbf{s}} = \begin{bmatrix} \dot{\mathbf{u}} \\ \dot{\mathbf{z}} \end{bmatrix} &= \mathbf{R}\dot{\mathbf{u}} \\ &= \begin{bmatrix} \mathbf{E} \\ \mathbf{T} \end{bmatrix}\dot{\mathbf{u}} \end{aligned} \tag{20}$$

Note that $\mathbf{E}$ is an identity matrix and $\mathbf{T}$ is an unknown matrix which needs to be proved. With respect to Equation (20), the vector $\dot{\mathbf{z}}$ can be expressed as follows:

$$\dot{\mathbf{z}} = \mathbf{T}\dot{\mathbf{u}} \tag{21}$$

Multiplying $\mathbf{J}_z$ with both sides of Equation (21) yields

$$\mathbf{J}_z\dot{\mathbf{z}} = \mathbf{J}_z\mathbf{T}\dot{\mathbf{u}} \tag{22}$$

Substituting Equation (22) into Equation (19) yields

$$-\mathbf{J}_u\dot{\mathbf{u}} = \mathbf{J}_z\mathbf{T}\dot{\mathbf{u}} \tag{23}$$

Hence

$$\mathbf{T} = -\mathbf{J}_z^{-1}\mathbf{J}_u \tag{24}$$

Finally, substituting Equation (24) into Equation (20) yields

$$\mathbf{R} = \begin{bmatrix} \mathbf{E} \\ -\mathbf{J}_z^{-1}\mathbf{J}_u \end{bmatrix} \tag{25}$$

Equation (25) completes the proof. □

4. Example: Kinematic and Dynamic Modelling of a Real Robot

In this section, the kinematic and dynamic modelling of a newly designed hybrid robot Class III are presented. The robot was designed and implemented with the purpose of handling material for a hot forging press shop floor. The 3D design of the robot and the robot prototype are shown in Figure 5a,b, respectively. The functional tests of the robot prototype and the numerical simulation of the kinematic and dynamic responses shows clearly the effectiveness and advantages of the method proposed in this study.
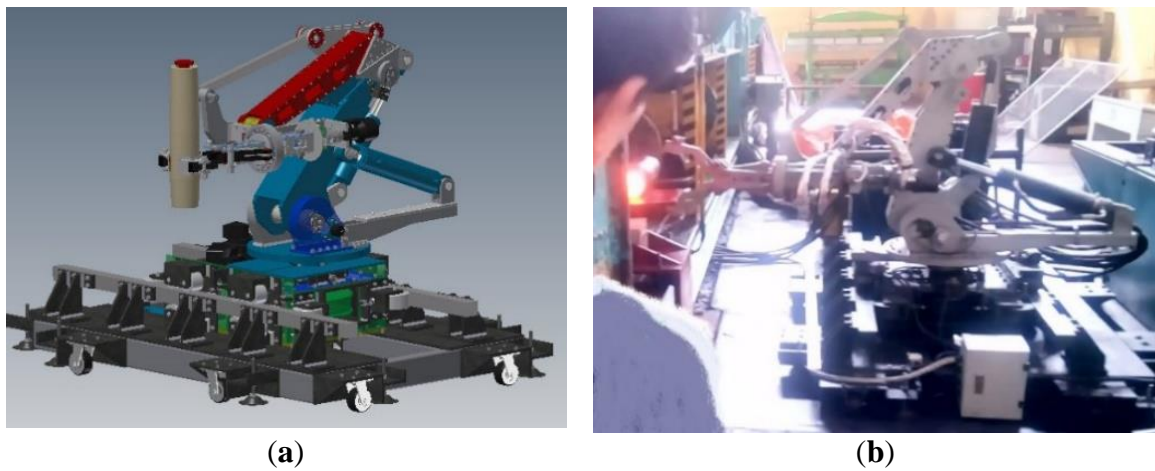
(a)   **(b)**

Figure 5. The forging robot: (**a**) The 3D design, and (**b**): The robot prototype.

The kinematic diagram of the robot is presented in Figure 6, which is designed with 4 serial links $\{l_i\}_{i=1 \div 4}$, and 4 local closed loops $\{\Theta_k\}_{k=1 \div 4}$ (Figure 7). The reference frame $O_0 x_0 y_0 z_0$ is located on the ground. The coordinate systems $O_1 x_1 y_1 z_1$, $O_2 x_2 y_2 z_2$, $O_3 x_3 y_3 z_3$ and $O_4 x_4 y_4 z_4$ are located on the serial links.
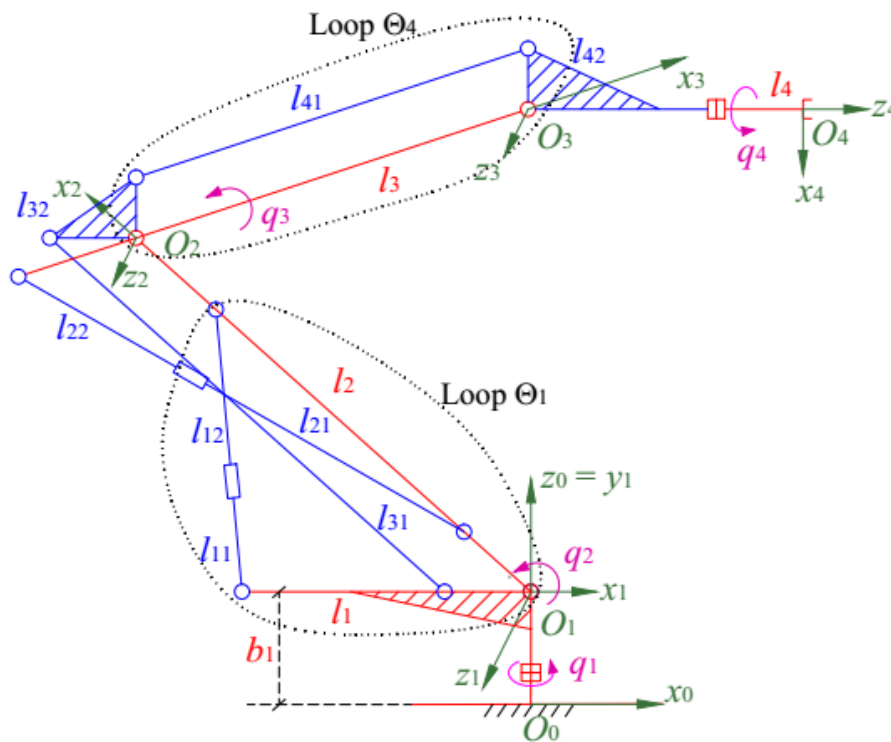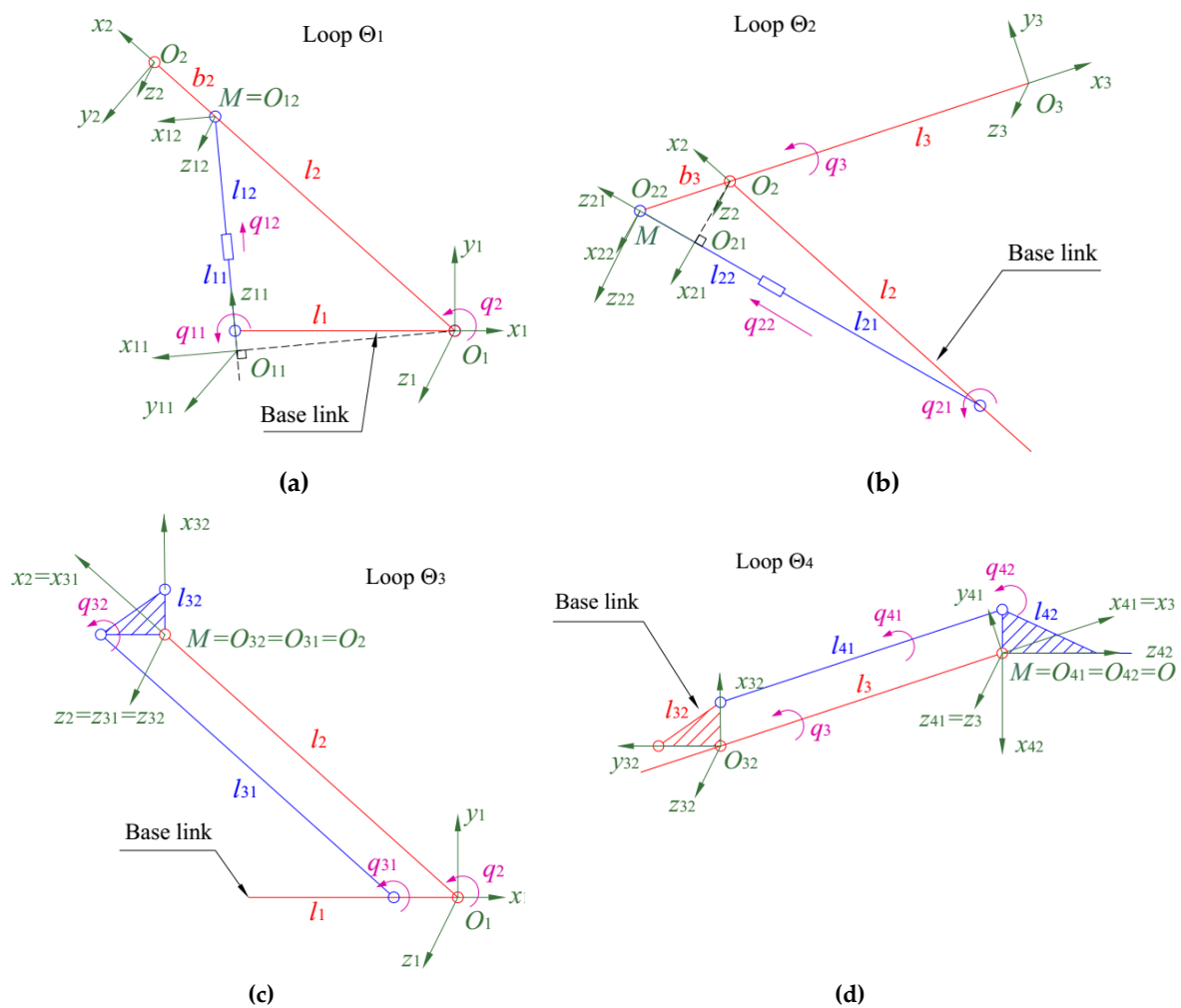

Figure 6. The kinematic chain of the forging robot.

Figure 7. The local closed-loop linkages of the forging robot: (**a**) Loop Θ_1, (**b**) Loop Θ_2, (**c**) Loop Θ_3, and (**d**) Loop Θ_4.

The joint variables of the main serial chain are $\mathbf{q} = \begin{bmatrix} q_1 & q_2 & q_3 & q_4 \end{bmatrix}^T$ (Figure 6).

Each local closed loop presented in Figure 7 is a four-bar linkage which is made up of two serial links (in red colour) and other two additional links (in green colour). Note that Θ_1 and Θ_2 are the loops of Type A; Θ_3 and Θ_4 are the loops of Type B.

The loop Θ_1 includes the link l_1, l_2, l_{11} and l_{12}. The joint variables of the loop are q_2, q_{11} and q_{12}. The loop Θ_2 consists of l_2, l_3, l_{21} and l_{22}. The joint variables of the loop are q_3, q_{21} and q_{22}. The loop Θ_3 consists of l_1, l_2, l_{31} and l_{32}. The joint variables of the loop are q_2, q_{31} and q_{32}. The loop Θ_4 consists of l_3, l_{32}, l_{41} and l_{42}. The joint variables of the loop are q_3, q_{41} and q_{42}. Table 1 presents the Denavit–Hartenberg notations of the four loops. Table 2 presents the dynamics parameters of the robot.

Table 1. The D-H notations of the four local closed loops.

Link	Loop Θ_1			Loop Θ_2			Loop Θ_3			Loop Θ_4		
	l_2	l_{11}	l_{12}	l_3	l_{21}	l_{22}	l_2	l_{31}	l_{32}	l_3	l_{41}	l_{42}
θ	q_2	q_{11}	0	q_3	q_{21}	0	q_2	q_{31}	q_{32}	q'_3	q_{41}	q_{42}
d	0	0	q_{12}	0	0	q_{22}	0	0	0	0	0	0
a	L_2	$-L_1 \cos q_{11}$	0	$L_3 - b_3$	$-L_2 \cos q_{21}$	0	L_2	L_2	0	$L_3 - b_3$	$L_3 - b_3$	0
α	0	$\frac{\pi}{2}$	$\frac{-\pi}{2}$	0	$\frac{-\pi}{2}$	$\frac{\pi}{2}$	0	0	0	0	0	$\frac{-\pi}{2}$

Table 2. Dynamic parameters of the robot.

Index j	Link	Mass Centre (m)			Mass (kg)
		x_C	y_C	z_C	
1	l_1	0	$b_1/2$	0	$m_1 = 81.3$
2	l_2	$L_2/2$	0	0	$m_2 = 50.6$
3	l_{11}	0	0	$L_{11}/2$	$m_3 = 25.6$
4	l_{12}	0	$L_{12}/2$	0	$m_4 = 5.70$
5	l_3	$L_3/2$	0	0	$m_5 = 58.4$
6	l_{21}	0	0	$L_{21}/2$	$m_6 = 25.6$
7	l_{22}	0	$L_{22}/2$	0	$m_7 = 5.70$
8	l_{42}	0	0	$L_{42}/2$	$m_8 = 37.7$
9	l_4	0	0	$L_4/2$	$m_9 = 73.1$
10	l_{31}	$L_2/2$	0	0	$m_{10} = 7.20$
11	l_{32}	$c_2/2$	0	0	$m_{11} = 12.9$
12	l_{41}	$L_3/2$	0	0	$m_{12} = 6.50$

The length of the links are given as follows: $L_1 = 0.7$; $L_2 = 0.7$; $L_3 = 0.8$; $L_4 = 0.2$; $L_{11} = 0.4$; $L_{21} = 0.4$; $L_{42} = 0.2$; $b_1 = 0.3$; $b_2 = 0.3$; $b_3 = 0.2$; $c_1 = 0.2$; $c_2 = 0.2$.

Note that $q_1, q_2, q_3, q_4, q_{11}, q_{12}, q_{21}, q_{22}, q_{31}, q_{32}, q_{41}$ and q_{42} are 12 generalized coordinates of the robot, in which

$\mathbf{u} = \begin{bmatrix} q_1 & q_{12} & q_{22} & q_4 \end{bmatrix}^T$ is the vector of 4 independent generalized coordinates,

$\mathbf{z} = \begin{bmatrix} q_2 & q_3 & q_{11} & q_{21} & q_{31} & q_{32} & q_{41} & q_{42} \end{bmatrix}^T$ is the vector of 8 dependent generalized coordinates and

$\mathbf{s} = \begin{bmatrix} \mathbf{u} & \mathbf{z} \end{bmatrix}^T$ is the vector of all 12 generalized coordinates of the robot.

Constraint equations

By using the formulation Equation (7), the constraint equations can be derived for 4 closed loops as follows:

$$f_1 = (L_2 - b_2)\cos q_2 + L_1 - (q_{12} + L_{11})\cos q_{11} = 0 \tag{26}$$

$$f_2 = (L_2 - b_2)\sin q_2 - (q_{12} + L_{11})\sin q_{11} = 0 \tag{27}$$

$$f_3 = b_3\cos q_3 - (L_2 - c_2) + (q_{22} + L_{21})\cos q_{21} = 0 \tag{28}$$

$$f_4 = b_3\sin q_3 + (q_{22} + L_{21})\sin q_{21} = 0 \tag{29}$$

$$f_5 = c_1\cos(q_2 + q_{32} - 3\pi/2) + L_2\cos q_2 - L_2\cos q_{31} + c_1 = 0 \tag{30}$$

$$f_6 = c_1\sin(q_2 + q_{32} - 3\pi/2) + L_2\sin q_2 - L_2\sin q_{31} = 0 \tag{31}$$

$$f_7 = -(L_3 - b_3)\cos(q_{32} + q_{41}) - (L_3 - b_3)\cos q_3 - c_1\sin(q_3 + q_{42}) - c_1\cos q_{32} = 0 \tag{32}$$

$$f_8 = (L_3 - b_3)\sin(q_{32} + q_{41}) + (L_3 - b_3)\sin q_3 - c_1\sin(q_3 + q_{42}) + c_1\sin q_{32} = 0 \tag{33}$$

Kinematics of the robot

By using the formulation Equation (1), the transformation matrix for the end-effector is calculated as follows:

$$\mathbf{H}_{04} = \mathbf{H}_{01}(q_1)\mathbf{H}_{12}(q_2)\mathbf{H}_{23}(q_3)\mathbf{H}_{34}(q_4) \tag{34}$$

Since Θ_3 and Θ_4 are the loops of Type B, by applying Equation (4), the matrices $\mathbf{H}_{23}(q_3)$ and $\mathbf{H}_{34}(q_4)$ are recalculated as follows:

$$\mathbf{H}_{23}(q_3) = \mathbf{H}_{2(31)}(q_{31})\mathbf{H}_{(31)(32)}(q_{32})\mathbf{H}_{(32)3}(q_3) \tag{35}$$

$$\mathbf{H}_{34}(q_4) = \mathbf{H}_{32(41)}(q_{41})\mathbf{H}_{(41)(42)}(q_{42})\mathbf{H}_{(42)4}(q_4) \tag{36}$$

Finally, the position of the end-effector $\mathbf{E} = \begin{bmatrix} x_E & y_E & z_E \end{bmatrix}^T$ is yielded as follows:

$$\begin{bmatrix} x_E \\ y_E \\ z_E \end{bmatrix} = \begin{bmatrix} \cos q_1(L_4 + L_{42} + (L_3 - b_3)\cos(q_2 + q_3) + L_2\cos q_2) \\ \sin q_1(L_4 + L_{42} + (L_3 - b_3)\cos(q_2 + q_3) + L_2\cos q_2) \\ (L_3 - b_3)\sin(q_2 + q_3) + L_2\sin q_2 + b_1 \end{bmatrix} \tag{37}$$

Note that

$$\cos q_2 = \frac{(q_{12} + L_{11})^2 - L_1^2 - (L_2 - b_2)^2}{2L_1(L_2 - b_2)} \tag{38}$$

$$\cos q_3 = \frac{-(q_{22} + L_{21})^2 + b_3^2 + (L_2 - c_2)^2}{2b_3(L_2 - c_2)} \tag{39}$$

Note that all the joint variables and the position of the end-effector in Equations (34)–(39) must be functions of time t. However, to simplify the representation of such the complex equations, the term (t) is truncated.

In order to verify the formulation of the kinematics model, the following numerical experiments were carried out:

1. Calculate the trajectory of the end effector $\mathbf{E}(t) = [x_E(t)y_E(t)z_E(t)]^T$, with the input data is given as $q_1(t) = \frac{\pi}{18} \times t$, $q_{12}(t) = 0.1 + 0.01 \times t$ and $q_{22}(t) = 0.15 + 0.005 \times t$. Figure 8 shows the curves of $\mathbf{E}(t) = [x_E(t) \ y_E(t) \ z_E(t)]^T$.
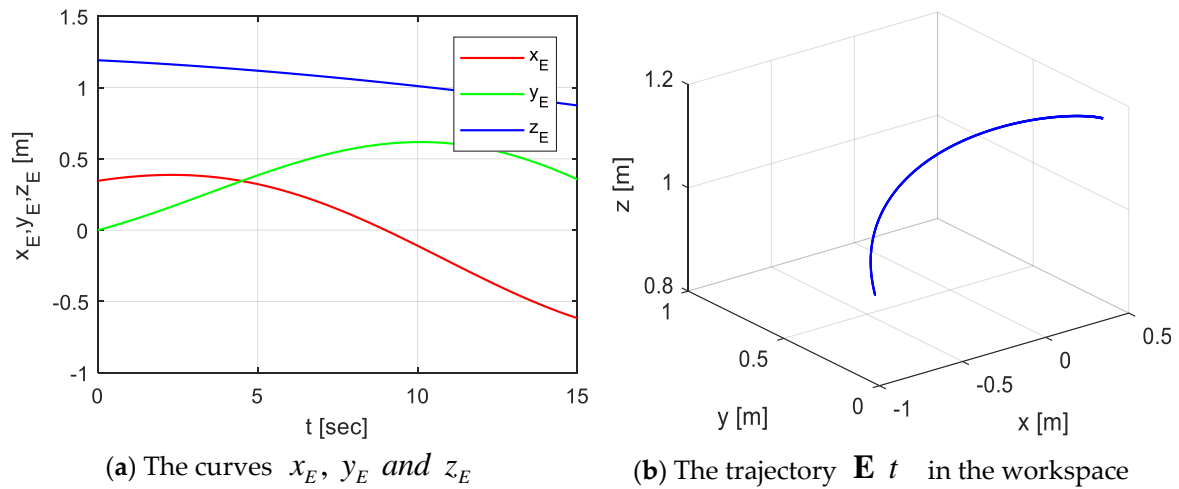

(**a**) The curves x_E, y_E *and* z_E (**b**) The trajectory $\mathbf{E}\ t$ in the workspace

Figure 8. The trajectory of the end-effector.

2. Take the data $\mathbf{E}(t) = [x_E(t)y_E(t)z_E(t)]^T$ obtained in Step 1 as the input for the inverse kinematic analysis, and calculate the displacement of the joints $q_1'(t)$, $q_{12}'(t)$ and $q_{22}'(t)$. The results are shown in Figure 9.

It is clearly shown in Figure 9 that the curves $q_1'(t)$, $q_{12}'(t)$ and $q_{22}'(t)$ obtained in Step 2 match exactly the given data $q_1(t)$, $q_{12}(t)$ and $q_{22}(t)$, respectively. This demonstrates and validates the proposed kinematic modelling method.

Dynamic Modelling and Analysis of the Robot

The dynamic equation of this robot can be derived directly by using the formulation Equation (17).

In order to formulate $\overline{\mathbf{M}}(\mathbf{s}, t), \overline{\mathbf{C}}(\mathbf{s}, \dot{\mathbf{s}}, t), \mathbf{G}(\mathbf{s}, t)$ and $\tau_q(t)$, the matrices $\mathbf{M}(\mathbf{s}, t)$, $\mathbf{C}(\mathbf{s}, \dot{\mathbf{s}}, t)$, $\mathbf{g}(\mathbf{s}, t)$ and $\mathbf{R}$ must be computed.
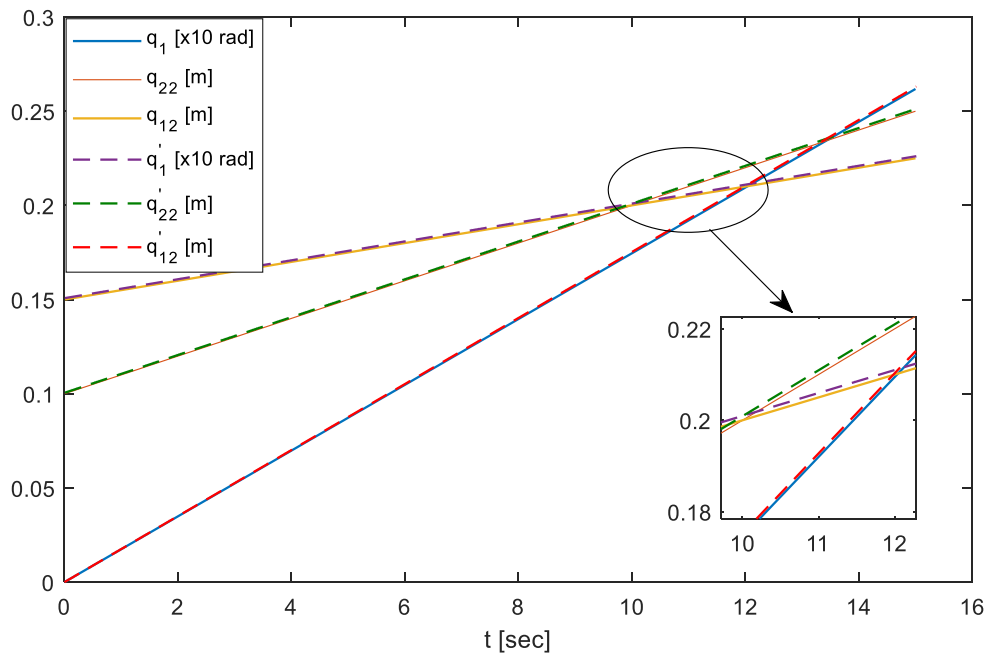
**Figure 9.** The displacement of the active joints.

In this manner, $\mathbf{M}(\mathbf{s}, t)$ can be calculated with Equation (11), where the masses m_j are given in Table 2, and the inertias $\mathbf{I}_j$ can be calculated based on the geometrical dimension of the links given in Table 2 as well. In Equation (11), the Jacobian matrices are calculated as $\mathbf{J}_{T_j} = \frac{\partial \mathbf{r}_{Cj}}{\partial \mathbf{s}}$ and $\mathbf{J}_{R_j} = \frac{\partial \boldsymbol{\omega}_j}{\partial \dot{\mathbf{s}}}$, where the centre of mass $\mathbf{r}_{Cj}$ and the angular velocity $\boldsymbol{\omega}_j$ are calculated and presented in the Appendix A. Based on all the components of $\mathbf{M}(\mathbf{s}, t)$, the matrix $\mathbf{C}(\mathbf{s}, \dot{\mathbf{s}}, t)$ is then calculated by using Cristoffel notation.

The component $\mathbf{g}(\mathbf{s}, t)$ is calculated with Equation (13), where the total potential energy of the robot, Π, is calculated and presented in the Appendix A also.

The matrix $\mathbf{R}$ is calculated with Equation (25), where the Jacobian matrices $\mathbf{J}_u$ and $\mathbf{J}_z$ are presented in the Appendix A, respectively.

Finally, all the terms of Equation (17) can be formulated properly that can be used for the dynamic analysis and the control law computation. In the following example, we demonstrate an inverse dynamic solution $\boldsymbol{\tau}_q = \begin{bmatrix} \tau_1 & F_{12} & F_{22} & \tau_4 \end{bmatrix}^T$ that was calculated with respect to a input data given as follows: $q_1(t) = \frac{\pi \times t}{18}$, $q_{12}(t) = 0.1 + 0.01t$, $q_{22}(t) = 0.15 + 0.005t$ and $q_4(t) = \frac{\pi \times t}{36}$. The responses of $\boldsymbol{\tau}_q = \begin{bmatrix} \tau_1 & F_{12} & F_{22} & \tau_4 \end{bmatrix}^T$ are shown in Figure 10.

It has shown that instead of the complex governing equations seen in Equation (10), the minimal form of the dynamic Equation (17) can be used directly for computation of the control (the inverse dynamic analysis) for the robot. In addition, analysing the dynamic model of a hybrid robot does not need to take into account the unknown Lagrangian Multipliers λ.
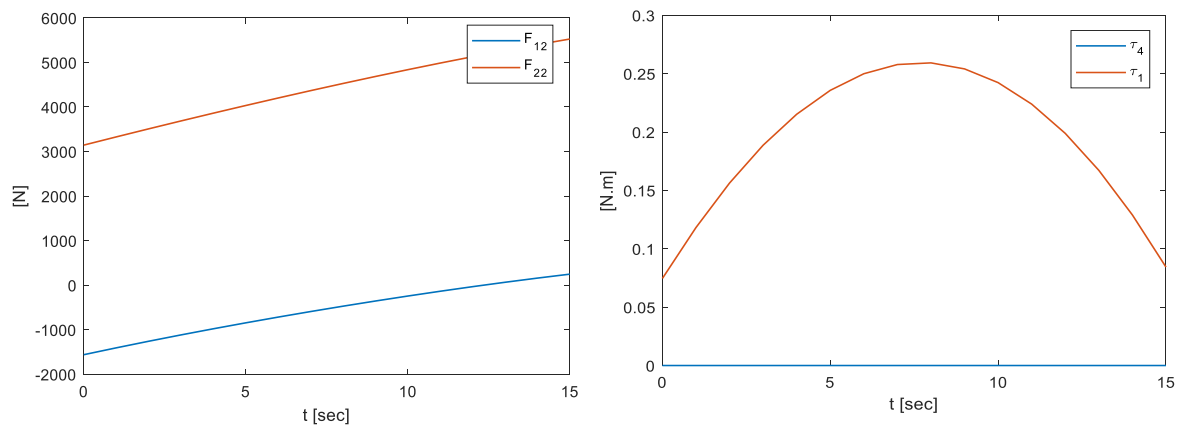
(a) The applied forces F_{12} and F_{22}

(b) The applied torques τ_1 and τ_4

Figure 10. The forces/torques applied on the active joints.

5. Conclusions

A new method for the kinematic and dynamic modelling for a class of hybrid robots was introduced in this study. The proposed method can be applied for the kinematic design of a robot mechanism composed of m local closed-loop linkages appended to a general n-link serial manipulator. In this manner, the kinematic equation for a generalized hybrid robot mechanism and the constraint equations due to the closed-loop linkages of a robot are derived effectively. Since a Lemma about the analytical relationship among the generalized velocities of a hybrid robot system was proven in a generalized case, the dynamic equation and constraint equations can be transformed into a minimal and compact form, so that the dynamics model of any hybrid robot can be formulated and analysed in an effective and simplified manner. Finally, to demonstrate and validate the proposed method, examples about the kinematic and dynamic modelling of a real robot are presented. It was shown clearly that, since the kinematic synthesis and the dynamic modelling of a hybrid robot take into account the constraint equations and the dynamic effects of all the local closed loops, the kinematics and dynamics model of a hybrid robot is formulated in a better and more accurate manner. In addition, since the method presented in this study was proposed and validated in a generalized case, it can be applied effectively for the kinematic and dynamic modelling of any individual hybrid robot Class III. In particular, when designing a new hybrid robot, the designers can follow all the steps of the kinematic design procedure presented in this paper to archive easily an optimal mechanism for the robot. The control law of the designing robot is then designed and simulated in an effective and useful manner by using the dynamic modelling procedure presented in this study as well. Therefore, the method proposed in this study is advantageous and plays an important role in the development of the hybrid robot products. All the experimental procedures for development of next versions of the robot prototype will be the future work of this study. The simulation of the kinematic and dynamic modelling of the hybrid robots having closed loops Type C and D will be the future study of the authors.

Author Contributions: Conceptualization, A.M.C. and C.D.N.; methodology, A.M.C. and C.D.N.; software, M.H.V.; validation M.H.V., A.M.C. and X.B.D.; formal analysis A.M.C., C.H.L. and M.H.V.; investigation, A.M.C., C.H.L. and T.A.N.; writing—original draft preparation, A.M.C.; writing—review and editing, C.H.L. and T.A.N.; project administration, A.M.C.; All authors have read and agreed to the published version of the manuscript.

Conflicts of Interest: The authors declare that there is no conflict of interest.

Appendix A

The centre of mass calculated for all the links of the robot

$$\mathbf{r}_{C1} = \begin{bmatrix} 0 \\ \frac{b_1}{2} \\ 0 \end{bmatrix}$$

$$\mathbf{r}_{C7} = \begin{bmatrix} \left(L_{21} + q_{22} - \frac{L_{22}}{2}\right)Cq_1 C(q_2 + q_{21}) + c_2 Cq_1 Cq_2 \\ \left(L_{21} + q_{22} - \frac{L_{22}}{2}\right)Sq_1 C(q_2 + q_{21}) + c_2 Sq_1 Cq_2 \\ \left(L_{21} + q_{22} - \frac{L_{22}}{2}\right)S(q_2 + q_{21}) + c_2 Sq_2 + b_1 \end{bmatrix}$$

$$\mathbf{r}_{C2} = \begin{bmatrix} \frac{L_2}{2} Cq_1 Cq_2 \\ \frac{L_2}{2} Sq_1 Sq_2 \\ \frac{L_2}{2} Sq_2 + b_1 \end{bmatrix}$$

$$\mathbf{r}_{C8} = \begin{bmatrix} Cq_1\left(\frac{L_{42}}{2} + (L_3 - b_3)C(q_2 + q_3) + L_2 Cq_2\right) \\ Sq_1\left(\frac{L_{42}}{2} + (L_3 - b_3)C(q_2 + q_3) + L_2 Cq_2\right) \\ (L_3 - b_3)S(q_2 + q_3) + L_2 Sq_2 + b_1 \end{bmatrix}$$

$$\mathbf{r}_{C3} = \begin{bmatrix} \frac{1}{2}L_{11}Cq_1 Cq_{11} - L_1 Cq_1 \\ \frac{1}{2}L_{11}Sq_1 Cq_{11} - L_1 Sq_1 \\ \frac{1}{2}L_{11}Sq_{11} + b_1 \end{bmatrix}$$

$$\mathbf{r}_{C9} = \begin{bmatrix} Cq_1\left(\frac{L_4}{2} + L_{42} + (L_3 - b_3)C(q_2 + q_3) + L_2 Cq_2\right) \\ Sq_1\left(\frac{L_4}{2} + L_{42} + (L_3 - b_3)C(q_2 + q_3) + L_2 Cq_2\right) \\ (L_3 - b_3)S(q_2 + q_3) + L_2 Sq_2 + b_1 \end{bmatrix}$$

$$\mathbf{r}_{C4} = \begin{bmatrix} \left(L_{11} + q_{12} - \frac{L_4}{2}\right)Cq_1 Cq_{11} - L_1 Cq_1 \\ \left(L_{11} + q_{12} - \frac{L_4}{2}\right)Sq_1 Cq_{11} - L_1 Sq_1 \\ \left(L_{11} + q_{12} - \frac{L_4}{2}\right)Sq_{11} + b_1 \end{bmatrix}$$

$$\mathbf{r}_{C10} = \begin{bmatrix} Cq_1\left(\frac{L_2}{2}Cq_2 - c_1\right) \\ Sq_1\left(\frac{L_2}{2}Cq_2 - c_1\right) \\ \frac{L_2}{2}Sq_2 + b_1 \end{bmatrix}$$

$$\mathbf{r}_{C5} = \begin{bmatrix} Cq_1\left(\frac{(L_3 - 2b_3)}{2}C(q_2 + q_3) + L_2 Cq_2\right) \\ Sq_1\left(\frac{(L_3 - 2b_3)}{2}C(q_2 + q_3) + L_2 Cq_2\right) \\ \frac{(L_3 - 2b_3)}{2}S(q_2 + q_3) + L_2 Sq_2 + b_1 \end{bmatrix}$$

$$\mathbf{r}_{C11} = \begin{bmatrix} Cq_1\left(L_2 Cq_2 - \frac{c_2}{2}\right) \\ Sq_1\left(L_2 Cq_2 - \frac{c_2}{2}\right) \\ L_2 Sq_2 + b_1 \end{bmatrix}$$

$$\mathbf{r}_{C6} = \begin{bmatrix} Cq_1\left(\frac{L_{21}}{2}C(q_2 + q_{21}) + c_2 Cq_2\right) \\ Sq_1\left(\frac{L_{21}}{2}C(q_2 + q_{21}) + c_2 Cq_2\right) \\ \frac{L_{21}}{2}S(q_2 + q_{21}) + c_2 Sq_2 + b_1 \end{bmatrix}$$

$$\mathbf{r}_{C12} = \begin{bmatrix} Cq_1\left(\frac{(L_3 - b_3)}{2}C(q_2 + q_3) + L_2 Cq_2\right) \\ Sq_1\left(\frac{(L_3 - b_3)}{2}C(q_2 + q_3) + L_2 Cq_2\right) \\ \frac{(L_3 - b_3)}{2}S(q_2 + q_3) + L_2 Sq_2 + c_1 + b_1 \end{bmatrix}$$

The angular velocities of the robot links

$$\boldsymbol{\omega}_1 = \begin{bmatrix} 0 \\ 0 \\ \dot{q}_1 \end{bmatrix} \qquad \boldsymbol{\omega}_2 = \begin{bmatrix} \dot{q}_2 Sq_1 \\ -\dot{q}_2 Cq_1 \\ \dot{q}_1 \end{bmatrix} \qquad \boldsymbol{\omega}_3 = \begin{bmatrix} \dot{q}_{11} Sq_1 \\ -\dot{q}_{11} Cq_1 \\ \dot{q}_1 \end{bmatrix}$$

$$\boldsymbol{\omega}_4 = \boldsymbol{\omega}_3 \qquad \boldsymbol{\omega}_5 = \begin{bmatrix} Sq_1(\dot{q}_2 + \dot{q}_3) \\ -Cq_1(\dot{q}_2 + \dot{q}_3) \\ \dot{q}_1 \end{bmatrix} \qquad \boldsymbol{\omega}_6 = \begin{bmatrix} Sq_1(\dot{q}_2 + \dot{q}_{21}) \\ -Cq_1(\dot{q}_2 + \dot{q}_{21}) \\ \dot{q}_1 \end{bmatrix}$$

$$\boldsymbol{\omega}_7 = \boldsymbol{\omega}_6 \qquad \boldsymbol{\omega}_8 = \boldsymbol{\omega}_1 \qquad \boldsymbol{\omega}_9 = \begin{bmatrix} \dot{q}_4 Cq_1 \\ \dot{q}_4 Sq_1 \\ \dot{q}_1 \end{bmatrix}$$

$$\boldsymbol{\omega}_{10} = \boldsymbol{\omega}_2 \qquad \boldsymbol{\omega}_{11} = \boldsymbol{\omega}_1 \qquad \boldsymbol{\omega}_{12} = \boldsymbol{\omega}_5$$

The potential energy of the robot

$$\begin{aligned}
\Pi &= \tfrac{1}{2}m_1 g b_1 + m_2 g\left(\tfrac{L_2}{2}Sq_2 + b_1\right) + m_3 g\left(\tfrac{1}{2}L_{11}Sq_{11} + b_1\right) \\
&+ m_4 g\left(\left(L_{11} + q_{12} - \tfrac{L_4}{2}\right)Sq_{11} + b_1\right) + m_5 g\left(\tfrac{(L_3 - 2b_3)}{2}S(q_2 + q_3) + L_2 Sq_2 + b_1\right) \\
&+ m_6 g\left(\tfrac{L_{21}}{2}S(q_2 + q_{21}) + c_3 Sq_2 + b_1\right) + m_7 g\left(\left(L_{21} + q_{22} - \tfrac{L_7}{2}\right)S(q_2 + q_{21}) + c_2 Sq_2 + b_1\right) \\
&+ m_8 g\left((L_3 - b_3)S(q_2 + q_3) + L_2 Sq_2 + b_1\right) + m_9 g\left((L_3 - b_3)S(q_2 + q_3) + L_2 Sq_2 + b_1\right) \\
&+ m_{10}g\left(\tfrac{L_2}{2}Sq_2 + b_1\right) + m_{11}g(L_2 Sq_2 + b_1) \\
&+ m_{12}g\left(\tfrac{(L_3 - b_3)}{2}S(q_2 + q_3) + L_2 Sq_2 + c_2 + b_1\right)
\end{aligned}$$

The Jacobian matrices $\mathbf{J}_u$ and $\mathbf{J}_z$

$$\mathbf{J}_u = \begin{bmatrix} 0 & Cq_{11} & 0 & 0 \\ 0 & Sq_{11} & 0 & 0 \\ 0 & 0 & Cq_{21} & 0 \\ 0 & 0 & Sq_{21} & 0 \\ 0 & 0 & 0 & 0 \\ 0 & 0 & 0 & 0 \\ 0 & 0 & 0 & 0 \\ 0 & 0 & 0 & 0 \end{bmatrix}$$

$$\mathbf{J}_z = \begin{bmatrix}
(L_2 - b_2)Sq_2 & -Sq_{11}(q_{12} + L_{11}) & 0 & 0 & 0 & 0 & 0 & 0 \\
-(L_2 - b_2)Cq_2 & Cq_{11}(q_{12} + L_{11}) & 0 & 0 & 0 & 0 & 0 & 0 \\
0 & 0 & -b_3 Sq_3 & -Sq_{21}(q_{22} + L_{21}) & 0 & 0 & 0 & 0 \\
0 & 0 & b_3 Cq_3 & Cq_{21}(q_{22} + L_{21}) & 0 & 0 & 0 & 0 \\
L_2 Sq_2 & 0 & 0 & 0 & 0 & -L_2 Sq_2 & 0 & 0 \\
c_1 - L_2 Cq_2 & 0 & 0 & 0 & 0 & L_2 Cq_2 & c_1 & 0 \\
0 & 0 & c_1 Cq_2 + (L_3 - b_3)Sq_3 & 0 & c_1 Cq_2 & 0 & (L_3 - b_3)Cq_3 - c_1 Cq_2 & (L_3 - b_3)Cq_3 \\
0 & 0 & -c_1 Sq_2 - (L_3 - b_3)Cq_3 & 0 & -c_1 Sq_2 & 0 & (L_3 - b_3)Sq_3 + c_1 Sq_2 & (L_3 - b_3)Sq_3
\end{bmatrix}$$

References

1.　Tanev, T.K. Kinematics of a hybrid (parallel–serial) robot manipulator. *Mech. Mach. Theory* **2000**, *35*, 1183–1196. [CrossRef]

2.　Cha, S.H.; Lasky, T.A.; Velinsky, S.A. Kinematic redundancy resolution for serial-parallel manipulators via local optimization including joint constraints. *Mech. Based Des. Struct. Mach.* **2006**, *34*, 213–239. [CrossRef]

3.　Gallardo-Alvarado, J. Kinematics of a hybrid manipulator by means of screw theory. *Multibody Syst. Dyn.* **2005**, *14*, 345–366. [CrossRef]

4.　Hu, B. Formulation of unified Jacobian for serial-parallel manipulators. *Robot. Comput. Integr. Manuf.* **2014**, *30*, 460–467. [CrossRef]

5.　Gallardo-Alvarado, J. Mobility analysis and kinematics of the semi-general 2 (3-RPS) series-parallel manipulator. *Robot. Comput. Integr. Manuf.* **2013**, *29*, 463–472. [CrossRef]

6.　Hu, B.; Yu, J. Unified solving inverse dynamics of 6-DOF serial–parallel manipulators. *Appl. Math. Model.* **2015**, *39*, 4715–4732. [CrossRef]

7.　Ibrahim, O.; Khalil, W. Inverse and direct dynamic models of hybrid robots. *Mech. Mach. Theory* **2010**, *45*, 627–640. [CrossRef]

8.　Lu, Y.; Dai, Z. Dynamics model of redundant hybrid manipulators connected in series by three or more different parallel manipulators with linear active legs. *Mech. Mach. Theory* **2016**, *103*, 222–235. [CrossRef]

9.　Lu, Y.; Dai, Z.; Ye, N. Stiffness analysis of parallel manipulators with linear limbs by considering inertial wrench of moving links and constrained wrench. *Robot. Comput. Integr. Manuf.* **2017**, *46*, 58–67. [CrossRef]

10.　Yuan, H.; You, X.; Zhang, Y.; Zhang, W.; Xu, W. A Novel Calibration Algorithm for Cable-Driven Parallel Robots with Application to Rehabilitation. *Appl. Sci. Theory* **2019**, *9*, 2182. [CrossRef]

11.　Cheng, H.H. Real-time manipulation of a hybrid serial-and-parallel-driven redundant industrial manipulator. *J. Dyn. Syst. Meas. Control* **1994**, *116*, 687–701. [CrossRef]

12.　Harib, K.H.; Ullah, A.S.; Moustafa, K.A.F. Optimal design for improved hybrid kinematic machine tools structures. *Procedia CIRP* **2013**, *12*, 109–114. [CrossRef]

13.　Kanaan, D.; Wenger, P.; Chablat, D. Kinematic analysis of a serial–parallel machine tool: The VERNE machine. *Mech. Mach. Theory* **2009**, *44*, 487–498. [CrossRef]

14.　Xu, P.; Cheung, C.F.; Li, B.; Ho, L.T.; Zhang, J.F. Kinematics analysis of a hybrid manipulator for computer controlled ultra-precision freeform polishing. *Robot. Comput. Integr. Manuf.* **2017**, *44*, 44–56. [CrossRef]

15.　Zeng, Q.; Ehmann, K.F. Design of parallel hybrid-loop manipulators with kinematotropic property and deployability. *Mech. Mach. Theory* **2009**, *71*, 1–26. [CrossRef]

16.　Pisla, D.; Szilaghyi, A.; Vaida, C.; Plitea, N. Kinematics and workspace modeling of a new hybrid robot used in minimally invasive surgery. *Robot. Comput. Integr. Manuf.* **2013**, *29*, 463–474. [CrossRef]

17.　Tönshoff, H.K.; Grendel, H.; Kaak, R. Structure and characteristics of the hybrid manipulator Georg V. In *Parallel Kinematic Machines*; Springer: London, UK, 1999; pp. 365–376.

18.　Guo, W.; Li, R.; Cao, C.; Gao, Y. Kinematics, dynamics, and control system of a new 5-degree-of-freedom hybrid robot manipulator. *Adv. Mech. Eng.* **2016**, *8*, 1687814016680309. [CrossRef]

19.　Nasseri, M.A.; Eder, M.; Eberts, D.; Nair, S.; Maier, M.; Zapp, D.; Knoll, A. Kinematics and dynamics analysis of a hybrid parallel-serial micromanipulator designed for biomedical applications. In Proceedings of the IEEE/ASME International Conference on Advanced Intelligent Mechatronics, Wollongong, Australia, 9–12 July 2013; pp. 293–299.

20.　Zeng, Q.; Fang, Y. Structural synthesis and analysis of serial–parallel hybrid mechanisms with spatial multi-loop kinematic chains. *Mech. Mach. Theory Manuf.* **2012**, *4*, 198–215. [CrossRef]

21.　Zeng, Q.; Fang, Y.; Ehmann, K.F. Design of a novel 4-DOF kinematotropic hybrid parallel manipulator. *J. Mech. Des.* **2011**, *133*, 121006. [CrossRef]

22.　Carbone, G.; Ceccarelli, M. A stiffness analysis for a hybrid parallel-serial manipulator. *Robotica* **2004**, *22*, 567–576. [CrossRef]

23.　Doan, Q.V.; Le, T.D.; Vo, A.T. Synchronization full-order terminal sliding mode control for an uncertain 3-DOF planar parallel robotic manipulator. *Appl. Sci. Theory* **2019**, *9*, 1756. [CrossRef]

24.　Acevedo, M.; Orvañanos-Guerrero, M.T.; Velázquez, R.; Arakelian, V. An Alternative Method for Shaking Force Balancing of the 3RRR PPM through Acceleration Control of the Center of Mass. *Appl. Sci.* **2020**, *10*, 1351. [CrossRef]

25. Kecskemethy, A.; Krupp, T.; Hiller, M. Symbolic processing of multiloop mechanism dynamics using closed-form kinematics solutions. *Multibody Syst. Dyn.* **1997**, *1*, 23–45. [CrossRef]

26. My, C.A.; Le, C.H.; Packianather, M.; Bohez, E. Novel robot arm design and implementation for hot forging press automation. *Int. J. Prod. Res.* **2018**, *57*, 4579–4593. [CrossRef]

27. Yan, C.; Gao, F.; Zhang, Y. Kinematic Modeling of a Serial–Parallel Forging Manipulator with Application to Heavy-Duty Manipulations. *Mech. Based Des. Struct. Mach.* **2010**, *38*, 105–129. [CrossRef]

28. Li, F.; Zhu, X.; Cao, J.; Yao, B. Kinematics Modeling and Workspace Analysis of a 5-DOF Hydraulic Manipulator. In Proceedings of the 5th International Conference on Control., Automation and Robotics (ICCAR), Beijing, China, 19–22 April 2019; pp. 713–718.

29. Bajpai, A.; Roth, B. Workspace and mobility of a closed-loop manipulator. *Int. J. Robot. Res.* **1986**, *5*, 131–142. [CrossRef]

30. Chung, G.J.; Kim, D.H.; Park, C.H. Analysis and Design of Heavy Duty Handling Robot. In Proceedings of the IEEE Conference on Robotics, Automation and Mechatronics, San Francisco, CA, USA, 7–10 April 1986; pp. 774–778.

31. Yang, C.; Wang, Y.; Yao, F. Driving performance of underwater long-arm hydraulic manipulator system for small autonomous underwater vehicle and its positioning accuracy. *Int. J. Adv. Robot. Syst.* **2017**, *14*, 1729881417747104. [CrossRef]

32. Kikuchi, H.; Niinomi, T.; Sato, M.; Matsumoto, Y.; Tokoro, Y. Heavy parts assembly by coordinative control of robot and balancing manipulator. *IFAC Proc. Vol.* **1984**, *17*, 2349–2354. [CrossRef]

33. Papadopoulos, E.; Mu, B.; Frenette, R. On modeling, identification, and control of a heavy-duty electrohydraulic harvester manipulator. *IEEE/ASME Trans. Mechatron.* **2003**, *8*, 178–187. [CrossRef]

34. Klimchik, A.; Pashkevich, A. Serial vs. quasi-serial manipulators: Comparison analysis of elasto-static behaviors. *Mech. Mach. Theory* **2017**, *107*, 46–70. [CrossRef]